J. Sound Vib. (1971) **15** (3), 397–420

MEASUREMENTS OF THE ACOUSTIC TARGET STRENGTHS OF FISH IN DORSAL ASPECT, INCLUDING SWIMBLADDER RESONANCE

B. S. McCartney and A. R. Stubbs

National Institute of Oceanography, Wormley, Godalming, Surrey, England

(*Received* 24 *September* 1970)

The need for measurements of the acoustic target strength of fish is discussed. The phenomenon of swimbladder resonance of small deep ocean fish is well known and is a useful means of estimating their sizes. For larger commercial fish in shallower seas the resonant frequency is much lower and resonance is very difficult to observe in the field. A method of observing and measuring the swimbladder resonance of a captive live fish in controlled conditions is described, and results on several gadoids are given. Reasons for the observed resonant frequencies being higher than predicted are given; the damping of resonance is high, which is expected. Application of these results to acoustic sizing at sea appears remote. They are relevant, however, to studies of low-frequency sound propagation, and the experimental technique is offered as a useful tool in physiological studies involving swimbladder function.

Measurements at higher frequencies in the diffraction and geometrical regions are also presented, resulting in an empirical equation for target strength as a function of length of the fish and wavelength. It is believed that this equation is useful for acoustic fish sizing using echo sounders at sea. The swimbladder is the major scatterer over the whole frequency range.

1. THE TARGET STRENGTH PROBLEM AND PREVIOUS WORK

When sound is incident on a fish some energy is dissipated by absorption and the rest is scattered in all directions. The proportion of re-radiated to incident intensity is dependent upon frequency, the incident and reflected angles, and the dimensions and mechanical properties of the fish structures. The number, complexity of shape, and relative motion of these structures in a living fish make it impossible to calculate the scattered field completely; even to estimate it with much confidence is difficult because the acoustic impedances of the various parts are uncertain and difficult to measure. Experimental determinations of target strength are thus essential. Over most of the useful spectrum little more than an order of magnitude agreement with the scattering calculated from simple geometrically shaped models can be expected.

Fortunately the number of parameters can be reduced to make a worthwhile practical investigation manageable. First, it is the back-scattered echo level which is invariably of interest and re-radiation in other directions need not be measured. Second, echo sounders detect fish principally at, or near, dorsal aspect, and we concentrate on this here, although this does not deny the need for measurements in azimuth at low elevations for forward search and scanning sonar applications. Third, measurements by Haslett [1] on whiting *Merlangius merlangus* (L.) showed that the dimensions of the acoustically important component of this species can be scaled as proportions of the fish length, L, leading to the useful idea [2] that the plot of acoustic back-scattering cross-section σ divided by L^2, *versus* L/λ (fish length/wavelength) should be the same for all whiting; in practice, this means that the

range of frequencies covered with each fish size, or *vice versa*, can be reduced. Caution is required when absorption losses become significant since these may not scale. Though many fish of other species have similar proportions to whiting, there are also some significant differences even within the gadoid family, particularly in the shape of the swimbladder.

The results of target strength measurements on *dead* fish in dorsal aspect by five sets of workers were plotted by Haslett in the normalized manner in Figure 1, taken from Figure 3 of reference [2], covering mainly the range $4 < L/\lambda < 20$, with some results down to $L/\lambda = 2$ and up to $L/\lambda = 60$. The main feature of this summary is the wide scatter, the extreme example being a factor of 5×10^3 between two results differing by only 20% in L/λ. This cannot be

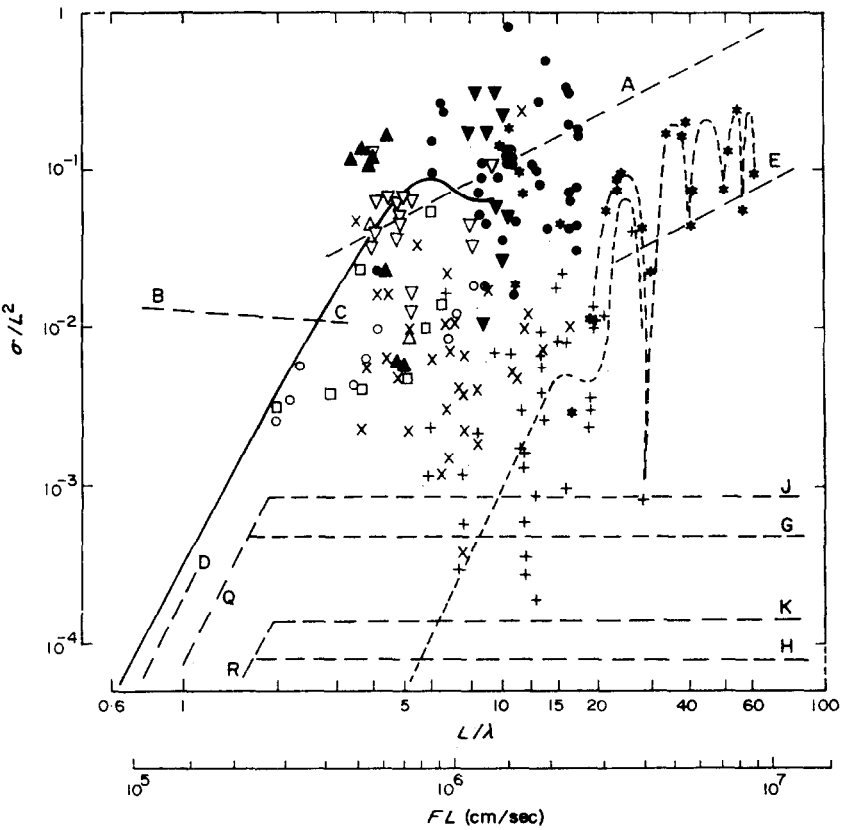

Figure 1. Normalized back-scattering cross-section σ/L^2 of fish in dorsal aspect. Results from six observers taken from Figure 3 of reference [2].

explained by selective absorption or resonance phenomenon, but rather indicates that scattering from two or more parts of the fish are interfering, causing large variations in re-radiation either at a fixed aspect as frequency is varied, or at a fixed frequency as aspect is varied. Variability in σ/L^2 tends to be worse at higher values of L/λ as each scattering component becomes more directional. Maximum values of σ/L^2 increase with L/λ, which is another indication of directivity. Values of σ/L^2 for smaller fish (at high frequencies) tend to be lower than the values of σ/L^2 from larger fish (at lower frequencies) having the same value of L/λ; this might indicate that increased absorption losses at the higher frequencies are becoming significant, in which case the sound may not be penetrating the fish flesh to reach other major scatterers such as the swimbladder and the backbone; alternatively, different experimental conditions make absolute comparisons difficult.

2. THE NEED FOR TARGET STRENGTH DATA

It would be desirable for acoustic systems to obtain information on the presence, position, quantity, size and species of fish in the sea. A knowledge of the acoustic back-scattering cross-section area of fish is required: (i) for the detectability specification of fishing sonars and echo-sounders; (ii) for the size determinations necessary for stock estimation; (iii) for classification of species by their echo properties.

2.1. DETECTABILITY

From Figure 1, for sounders aiming to detect a single fish and operating within $4 < L/\lambda < 20$, the minimum detectable target at maximum range may be specified as $\sigma = 10^{-4}L^2$, though to achieve $\sigma = 10^{-3}L^2$ would allow detection in well over 90% of occasions.

2.2. SIZING

Cushing [3] has obtained a statistical estimate of fish population by converting target strengths observed at sea at a fixed frequency into the corresponding distribution of fish sizes. For this purpose the most convenient form for representing the data is an empirical equation relating target strength, T, to L and λ; T is defined by

$$T = 10\log_{10}(\sigma/4\pi). \tag{1}$$

This has been done in section 6 below using our own data and that from Figure 1, in a manner similar to that used by Love [4] for the maximum side-aspect target strength.

It is now widely accepted [5–8] that the peaks in the volume scattering coefficient spectra of many sonic scattering layers in the deep ocean are due to the resonances of fish swimbladders. Since the resonant frequency is a function of the swimbladder volume and this in turn is directly related to the size of the fish, measurement of the resonant frequency is an attractive direct method of fish sizing, being independent of equipment gain levels and fish aspect.

Resonance occurs because, like a gas bubble, the swimbladder is a compliance whose acoustic loading at long wavelengths is predominantly the inertia of the surrounding water. For a bubble of radius a the resonant frequency, f_0, is given by Minnaert's formula [7]

$$f_0 = \frac{1}{2\pi a}\sqrt{\frac{3\gamma P}{\rho}}, \tag{2}$$

where γ is the ratio of specific heats for the gas, P is the absolute static pressure and ρ is the water density.

For deep scattering layers between 100 and 1000 m depth, resonant frequencies occur between 3 and 20 kHz, and it is estimated that the fish responsible are between 10 and 1 cm in length. If the sizes of such small fish can be estimated at 1000 m depth, it seems reasonable to enquire whether the sizes of larger fish of commercial interest found at the shallower shelf depths may also be determined acoustically. For fish of length between 1 m and 10 cm, resonant frequencies are expected to fall in the range 100 Hz to 1 kHz. After some experiments [9, 10] with wide-band sources on fish shoals located at sea, it was realized that insufficient was known about the effects of acoustic interaction between fish within the shoal, so that the aggregated scattering from the shoal did not necessarily have the same spectral form as that from a single fish, and this itself was insufficiently well known. This contrasts with the case of the deep scattering layers, in which the packing density is too small for interaction to be troublesome, and where at long wavelengths the individual scatterer may be represented fairly well by a moderately damped spherical gas bubble. In sections 3 to 5 we have determined experimentally, for single *live* fish in controlled conditions, the relationship between length,

depth, and resonant frequency and the damping of resonance. It should be noted that the work complements theoretical studies by Weston [7] and Andreeva [6] who predict large damping for resonance at shallow depths.

2.3. CLASSIFICATION

The echo sounder has been used by the fishing industry for 30 years to detect fish, and reports [11, 12] of fishermen able to identify successfully many of the echo traces are too numerous to be dismissed. In addition to their echo sounder information, the fishermen are undoubtedly using local knowledge of the grounds and past experience of catches. It is not easy to assess the relative contributions of the acoustic data and fishing knowledge to classification. The need to spend perhaps 10 months each year on commercial fishing vessels extracting subjective information from busy skippers without getting in the way is a daunting prospect. It is therefore not too surprising that there does not appear to have been any scientific investigation of these abilities possibly leading to changes of echo-sounder design for improved classification.

The few attempts [13–15] to create acoustic classification systems have employed wide bandwidths to obtain echo spectra expected to be characteristic of the target, but results with these are too sparse to be assessed at the present time.

3. SWIMBLADDER RESONANCE EXPERIMENTS

The conventional method of measuring target strength is to transmit a pulse several cycles long of known intensity and to measure the range and amplitude of the returned echo, which is separated in time from the transmission pulse. When this is attempted with small scatterers at very low frequencies, difficulties arise because the pulse, being several cycles long and therefore several wavelengths long, is still being transmitted when the received echo is returned, unless the fish is at a great range; then the signal level may be so low that detection is poor against the background noise, which is usually high at low frequencies. A short impulsive wide-band source would be attractive, allowing determination of the spectral response in one pulse, but all sufficiently energetic sources available to date in this frequency band have rather large, long and unreliable tails to their pulses so that the same objection as for the mono-frequency pulse applies.

Objects smaller than a wavelength may be considered to consist of connected lumped parameters such as masses, compliances and loss resistances and if the complex mechanical impedance of an object is known, then the target strength at low frequencies can in principle be estimated. Several techniques [16] using enclosed volumes or tubes are available for the measurement of complex acoustic compliance but the technique we have adopted is a free-field method in which corrections for a chamber are not required and so that plane incident waves can be used.

The method shown in Figure 2 was employed from *F.R.S. Mara* moored in Loch Torridon and operating as nearly as possible as a "silent" ship. The basic principle is to measure the acoustic waveform at some distance from a wide-band sound source with a hydrophone close by the fish and then to repeat the measurement after removing the fish. After considerable difficulty with the technique in 1967, using pulses from a pneumatic sound source and using omnidirectional spherical hydrophones, a more successful arrangement was found in 1968 using a CW source (a J11 underwater loudspeaker manufactured by Empire Scientific Corporation, U.S.A.), and a ceramic ring hydrophone 10 cm in diameter, inside which the fish is centrally placed. The signal from a Brüel and Kjær B.F.O., sweeping from 20 Hz to 20 kHz, is amplified and fed to the loudspeaker. The amplitude of the received hydrophone signal $|v|$ is recorded on an ink-pen recorder whose paper drive is synchronized mechanically

to the B.F.O. The second ring hydrophone 1 m away is used to monitor the source level transmitted, whilst the output of the first is recorded with and without a fish present in the cage. This cage, made from moulded plastic mesh (trade name Netlon), was found to be

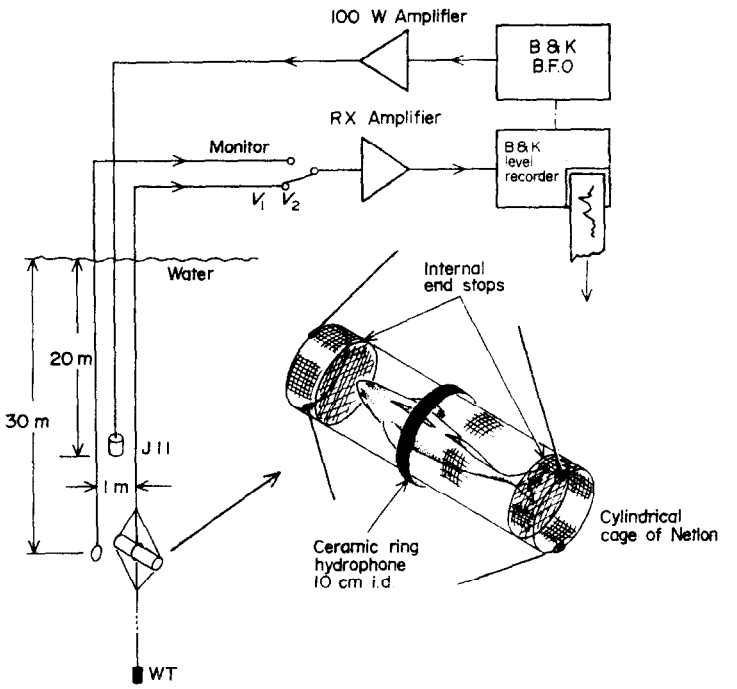

Figure 2. CW experiment from *F.R.S. Mara*, moored in Loch Torridon.

better than a polythene bag, used in some of the earlier experiments; the fish could be inserted easily into the cage, its movement restricted, yet water could flow to allow respiration and it did not trap air bubbles. The acoustic interference from the cage was negligible below 5 kHz.

By definition,

$$\sigma = 4\pi R^2 \overline{p_s^2}/\overline{p_i^2}, \tag{3}$$

where $\overline{p_s^2}$ is the mean square scattered pressure at a distance R from the fish and $\overline{p_i^2}$ is the mean square pressure incident on the fish. Strictly, equation (3) applies only in the far field of the scattered pressure, i.e. $R > \lambda$. With the geometry of this experiment, $R = 5$ cm, p_i is a plane wave incident "edge on" to the ring hydrophone, with sensitivity S_p, whilst p_s is a wave assumed to be spreading spherically from the centre of the ring, whose sensitivity in this case is S_s; the relationship between S_p and S_s is frequency dependent in the band of interest (Appendix I and Figure A1). For a spherically spreading wave the pressure at $R < \lambda$ is proportional to far-field pressure, but if the scattered wave is not spherical there will in general be a frequency-dependent relation between the pressure measured and the required far-field value.

Using subscript 1 when the fish is present and 2 when absent, we have the hydrophone voltages

$$v_1 = S_p . p_i + S_s . p_s, \tag{4}$$

$$v_2 = S_p . p_i. \tag{5}$$

When (3), (4) and (5) are combined,

$$\sigma = 4\pi R^2 (S_p/S_s)^2 [\overline{(v_1 - v_2)^2}/\overline{v_2^2}]; \tag{6}$$

v_1 and v_2 are strictly both vectors, but since they are not available simultaneously subtraction is impossible from records of $|v_1|$ and $|v_2|$, unless phase differences are known. One possibility is to assume that the monitor hydrophone voltage approximates v_2, since it is some way from the scatterer, and then use a phase meter at fixed frequencies sequentially. This method was employed once, but a more convenient method is available because $S_s \gg S_p$ and hence, particularly around resonance, $v_1 \gg v_2$, so that regardless of phase $\overline{(v_1 - v_2)^2} \simeq \overline{v_1^2}$ and we can write, from equations (1) and (6), since $\overline{v_1^2} \propto |v_1|^2$,

$$T \simeq 20 \log_{10}(R.S_p/S_s) + 20 \log_{10} |v_1/v_2|. \tag{7}$$

The second term is obtained directly from the level recordings and the first is a calibration factor. In practice, a reasonable approximation results if $20 \log_{10} |v_1/v_2|$ exceeds 10 dB. Then the phase angles are such that below resonance T is overestimated by less than 1·8 dB, at resonance T is overestimated by less than 0·4 dB, and above resonance T is underestimated by less than 1·3 dB. Most of the results here are uncalibrated plots but do give resonant frequency and damping with acceptable error in most cases. Calibrated plots are included in the summary, Figure 11, for three fish.

Cod, *Gadus morhua* (L.), ling, *Molva molva* (L.), pollack, *Pollachius pollachius* (L.), and coalfish (or saithe), *Pollachius virens* (L.) were caught on hand lines, and then either brought to the surface, or removed from the hook at depth by divers and placed directly into the keep cage at 30 m. The latter is the most satisfactory where possible, since there is a much reduced chance of damage to the swimbladder. At the end of the experiment three fish were brought to the surface, killed, measured and the state of the swimbladder examined; two fish were dissected *in situ* at 30 m, three fish escaped during handling, and one was kept alive indefinitely. An experiment with herring, *Clupea harengus* (L.), caught in a drift net failed because of the poor condition of the fish which died during the experiment.

4. RESULTS OF RESONANCE MEASUREMENTS

The results for three cod, plotting $20 \log |v_1/v_2|$ *versus* frequency, are shown in Figure 3. The main feature of these results, in which resonance is clearly demonstrated, is that the 35 cm cod has a lower resonance than the 32 cm cod, but that the resonance of the 39 cm cod, which would be expected to be even lower, fell in between the two; this fish was later found

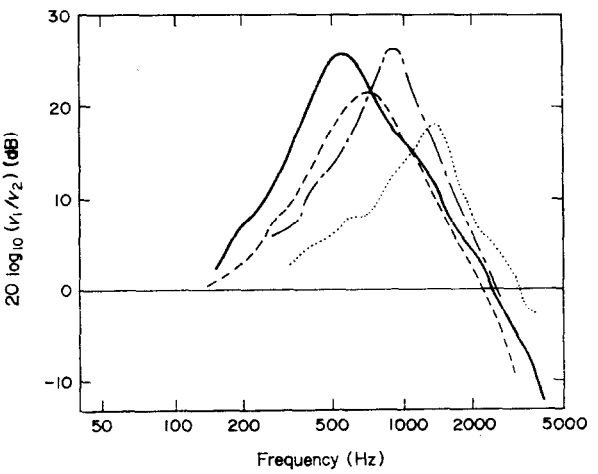

Figure 3. Resonance curves for cod. Cod A: 32 cm, ——, 14.20 26 September, ..., 06.50 27 September; cod B, 39 cm, – – –, swimbladder ruptured; cod C, 35 cm, ——.

to have a ruptured swimbladder, which might explain the greater losses and the higher resonance due to lost gas.

Figure 4 shows how the resonant frequency of the 32 cm cod increased by 50% with time, reaching a stable value (which was then held overnight), and shows the corresponding change in swimbladder volume estimated from equation (2). This could be slow loss of gas from a ruptured bladder or, more speculatively, perhaps because the fish was absorbing oxygen from its swimbladder during the period up to 19.00 hours, after which the residual gas was mainly nitrogen. This experiment was one of the earliest using a polythene bag, pierced by several small holes which may have been insufficient to allow adequate water flow for respiration.

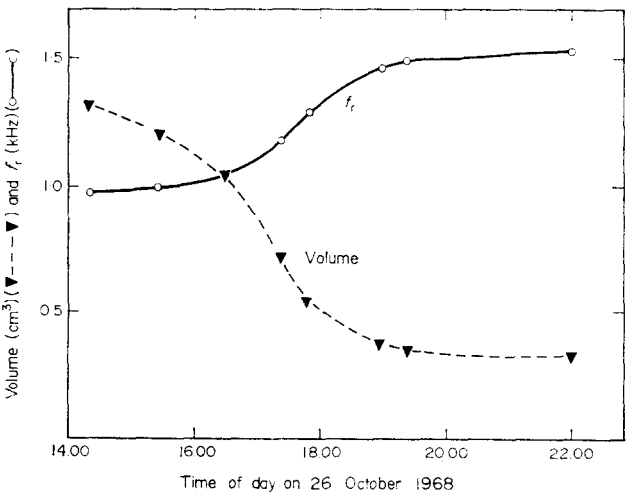

Figure 4. Variation in resonant frequency of cod A of Figure 3 with time and approximate swimbladder volume changes. o—— o, f_r; ▼ ---▼, volume.

The estimate of volume is not too accurate due to uncertainties about the effects of tissue elasticity and shape, discussed further below.

The results of Figure 5 were obtained from the largest fish used, which was a 55 cm ling, and show the resonance at 500 Hz with, in this case, a small decrease in frequency overnight.

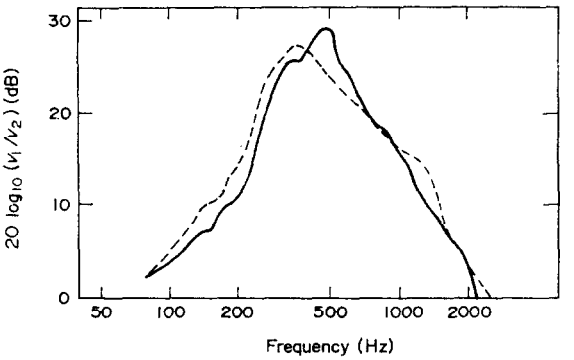

Figure 5. Resonance curves for the 55 cm ling on two consecutive days. ——, 13.15 hr 17 October; – – –, 09.00 hr 18 October.

The results for a 35 cm pollack in Figure 6 show increases in resonant frequency and in Q, or decrease in damping, as the fish is placed deeper, and then a further large increase in Q

after the fish is killed *in situ* and the gut below the swimbladder removed, leaving the swimbladder intact. Since the Q doubled when the gut was removed it follows that half the damping was previously due to the viscous losses within the gut. The accuracy in resonant frequency is not really good enough to judge whether the mass loading on the swimbladder is reduced when the gut is replaced by the less dense water.

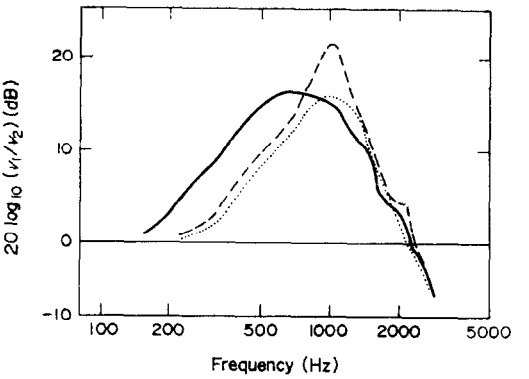

Figure 6. Resonance curves for the 35 cm pollack. ——, Alive at 30 m; ....., alive at 40 m; – – – –, dead at 40 m and gut removed.

The results in Figure 7, for coalfish, indicate again increased damping when the swimbladder is burst, and a slightly higher resonant frequency. When the fish with an intact swimbladder is raised from 30 to 20 m and then to 10 m, quickly enough to prevent gas resorption at the new static pressures, the resonant frequency drops and the damping becomes larger suggesting that losses within extended tissue are responsible.

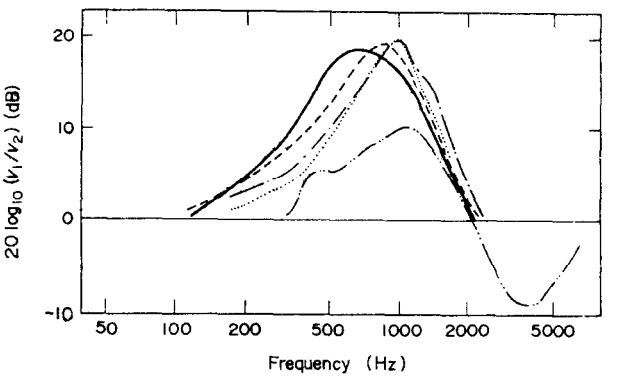

Figure 7. Resonance curves for coalfish. Coalfish A, 29·5 cm: ——, Dead at 10 m; – – – –, dead at 20 m; —·—, dead at 30 m; ..... alive at 30 m. Coalfish B 32 cm: —··— ruptured swimbladder, at 30 m.

The presence of the fish with a swimbladder effectively alters the sensitivity of the hydrophone to incident acoustic waves, converting plane waves to spherical waves, especially at resonance. In Plate 1 the ambient noise level recordings in third-octave bands with and without the pollack are shown. The reduction in sensitivity at the ring resonance at 6 kHz is evident and the increase between 450 and 2000 Hz, peaking at the resonance around 800 Hz, is due to the resonance of the pollack.

A third method of demonstrating swimbladder resonance is illustrated by Plate 2. It shows the waveforms obtained 30 m below an air-gun sound source with a ring hydrophone. The lower trace, **B**, is in the absence of the fish and shows that the air-gun waveform is

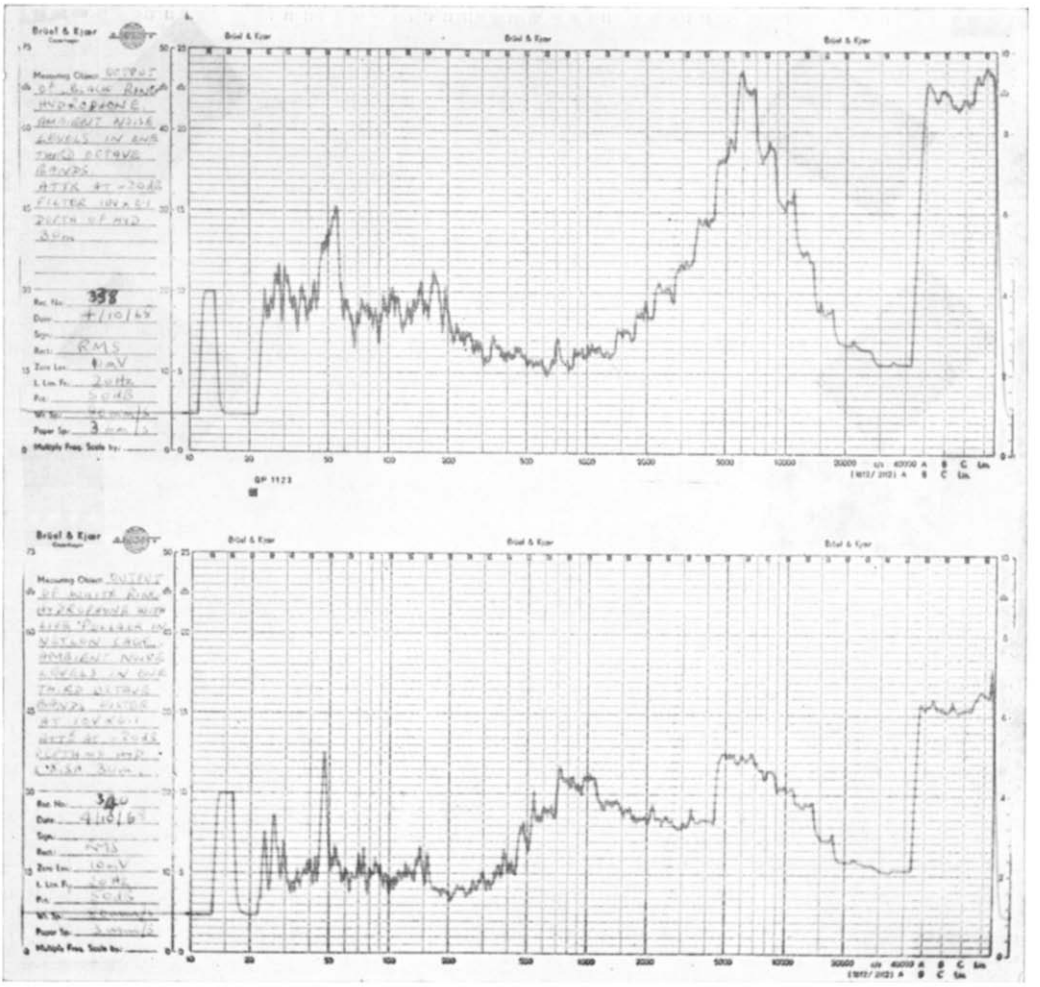

Plate 1. Ambient noise level recordings in third-octave bands using the ring hydrophone at 30 m. Upper record: without fish. Lower record: with a pollack inside the ring.

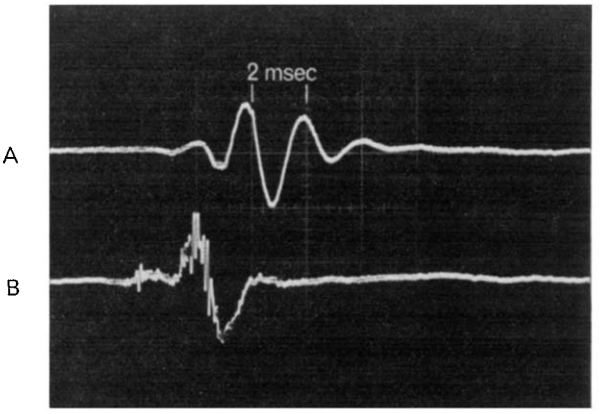

Plate 2. Voltage waveforms from the ring hydrophone 30 m below the air-gun, a pneumatic sound source. A, with ling inside the ring; B, without fish.

(*facing p.* 404)

essentially one cycle at 400 Hz, preceded by a small pre-pulse. The high frequency waveform superposed is due to the high sensitivity of the ring hydrophone at its resonant frequency around 6 kHz. The upper trace, A, shows that the high frequency ring resonance is suppressed due to the pressure release effect of the swimbladder above resonance and the waveform is mainly a heavily damped pulse at 500 Hz, the resonance of the ling swimbladder. Spectrum analyses of these waveforms followed by division of the level of A by the level of B at the same frequency yields the same spectral shape of $|v_1/v_2|$ as the CW technique.

5. DISCUSSION OF RESONANCE EXPERIMENTS

The measured values of the resonant frequencies, Table 1, of all the fish are higher than one would expect on the basis of representing a fish swimbladder by a spherical bubble of the

TABLE 1

	Fish							
	Coal-fish A	Coal-fish B	Coal-fish D	Ling	Cod A	Cod B	Cod C	Pollack
Length L (cm)	29·5	32	30	55	32	39	35	35
Handling procedure	A	A	B	A	A	C	A	D
Swimbladder condition	I	R_0	?E	I	?E	R_{30}	?E	I
Swimbladder length (cm)	8·9	10·4	—	—	—	—	—	14·5
Aspect ratio at surface	6·4	10·0†	—	—	—	—	—	8·5
Aspect ratio at 30 m	8·2	—	—	—	—	—	—	12·0
Measured volume at surface (ml)	10·1	8·0‡	—	—	—	—	—	11·0
Estimated volume of swimbladder at 30 m (ml)	4·6	—	—	17§	—	5·9§	14·7§	5·5
$V_N = 4{\cdot}1 \times 10^{-4} L^3$ (ml)	10·5	13·4	11·1	68·2	13·4	24·3	17·6	17·6
f_r (at 10 m) Hz	600	—	—	—	—	—	400	—
(at 20 m)	830	—	—	400	—	550	470	—
(at 30 m)	950	1000	800	500	910	700	560	766
(at 40 m)	—	—	—	—	—	—	—	921
(at 55 m)	—	—	—	—	—	—	—	1120
D_T (±2 m of water)	15	—	—	2	—	1	8–15	2
Q at 30 m	2·5	~1	~1	2·5	3·5	1·8	2·0	~1
$f_r L$ at 30 m (Hz m)	280	320	240	275	290	270	200	270
f_r at 30 m calculated from equation (10)	898	—	—	—	—	—	—	791

Handling procedures

- A Fish removed from hook at surface, transported across Loch to ship at surface pressure in tank, lowered to working depth in stages and allowed time to equilibrate. After experiment raised to surface for examination (or escape!).
- B Fish removed from hook at depth, transported across Loch at working depth to site.
- C As A but examined *in situ* at 30 m.
- D As B but examined *in situ* at 30 m.
- E Escaped.
- I Intact.
- R_0 Ruptured at surface.
- R_{30} Ruptured at 30 m.
- † High because of rupture.
- ‡ Low because of rupture.
- § Calculated from equation (10) using measured f_r.

same volume required to give the fish neutral buoyancy. For a marine fish, the radius of such a bubble would be from [1]

$$a = 0{\cdot}043\, L. \tag{8}$$

From equations (2) and (8), using $\gamma = 1{\cdot}40$ (oxygen) and $\rho = 1{\cdot}08$ g/cm^3 [17], for fish flesh which has greater influence than the water due to its proximity, we have

$$f_r = 23{\cdot}0\, L^{-1}(D_f + 10)^{1/2}, \tag{9}$$

where f_r is in Hz, L in metres and D_f is the depth of the fish in metres. Thus for $D_f = 30$ m, $f_r L = 145$. Observed values are 40–100% higher. The validity of equation (8) for these fish is not known. Also the swimbladder may not be fully inflated, or it may be under tension, or the effect of shape may be more than predicted. These uncertainties pointed to the need for some control experiments with artificial targets and, for this, slightly inflated toy balloons were stretched to approximate prolate spheroids.

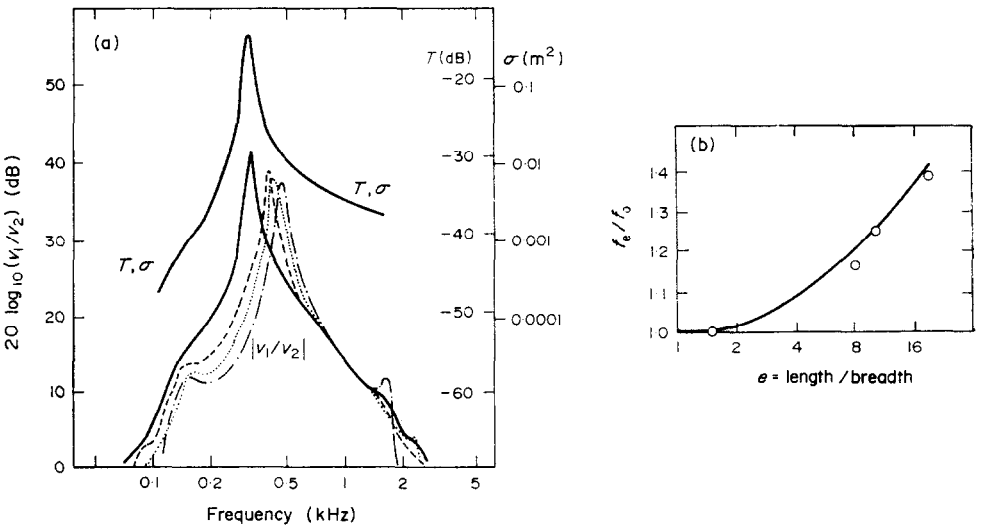

Figure 8. (a) Resonance curves of constant volume balloon at various elongations, together with the calibrated target strength and σ of the nearly spherical balloon. ——, $e = 1{\cdot}4$; – – – –, $e = 8$; ……, $e = 10$; —·—, $e = 20$.

(b) Ratio of the resonant frequency of an elongated balloon to that of a spherical balloon having the same volume. ——, theoretical ratio for prolate spheroid (Weston [7]).

The results for a constant volume balloon at four values of length to diameter ratio, e, are given in Figure 8(a). The proportional increase in resonance, which is now at a high Q of around 10 due to reduced tissue losses, is plotted in Figure 8(b) as a function of e. Though they are not exactly prolate spheroids, the agreement with Weston's calculations [7] is quite close. The curve in Figure 8(a) labelled σ is the acoustic back-scattering cross-section after sensitivity corrections have been applied, for the nearly spherical balloon of radius 1·9 cm at 30 m. The resonant scattering section is very close to the theoretical value for a bubble of this size with a Q of 10. The balloon experiments confirm that the experimental technique is valid and that the high resonant frequencies of fish are genuine, and moreover for the typical length-to-diameter ratios of fish swimbladders, Table 1, it is clear that elongation can account for only 20–30% of the increase in $f_r L$.

Unfortunately, detailed measurements of the swimbladder sizes and shapes at the surface are available for only two of the intact fish, the coalfish A and the pollack; it is most significant that these swimbladder volumes at the surface, calculated from the measured dimensions, are less than the nominal neutral buoyancy volume $4{\cdot}1 \times 10^{-4}\, L^3$ which is based upon the

dimensions of whiting [1] and the average specific gravity of fish flesh. The divers reported on several occasions that fish appeared to be "heavy" at 30 m depth, where the swimbladder volumes must have been even lower.

In general, tension in the swimbladder tissues has three major effects on resonance, as discussed in Appendix II; briefly, these are (i) an increase in static gas pressure over the external hydrostatic pressure, (ii) an increase in the overall dynamic stiffness to radial vibration and (iii) an increase in viscous damping. The first two tend to increase the resonant frequency and together may be represented by an excess internal pressure, equivalent to D_T metres of water pressure, which will depend on the elasticity of the swimbladder, the mass of gas and the unextended size of the bladder. The apparent values of D_T were obtained for five fish (Table 1) and for the balloon as follows. Changes in resonant frequency of a constant

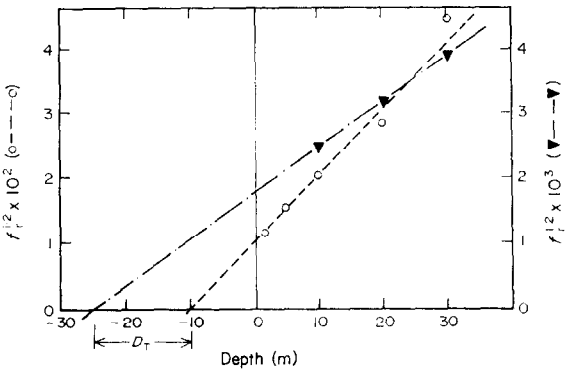

Figure 9. Variation in resonant frequency with depth for a coalfish and the spherical balloon, to determine D_T. ▼——▼, Coalfish; o——o, spherical balloon.

mass of gas have a $\frac{5}{6}$th power law dependence on absolute pressure, so that a plot of $f_r^{1\cdot2}$ against depth should be a straight line [7], if D_T is constant. The results for a balloon and a coalfish are shown in Figure 9. The excess pressure in the balloon is very small; this fact was confirmed by a manometer measurement. For the coalfish, the straight line may be fortuitous since the accuracy of f_r is poor, when measured from plots of $\log_{10}|v_1/v_2|$; accuracy can be improved by manually tuning for the resonant peak using a voltmeter for v_1, and a frequency meter connected to the B.F.O. For the ruptured cod B, D_T was very small as would be expected; for cod C, the plot was not linear and it is estimated that $D_T = 8$ m at $D_f = 30$ m and $D_T = 15$ m at $D_f = 10$ m. The value of D_T for the ling is not accurate as frequencies at only two depths were available; but for the pollack, frequencies at greater depths than 30 m give a good line with $D_T = 2$ m. From Appendix II it may be seen that a straight line can only be expected if the static excess is zero, in which case

$$D_T = D_t = 4\mu_1(t/\gamma a) \times 10^{-5}$$

and

$$f_r = (2\pi a)^{-1}\rho^{-1/2}[3\gamma P + 4\mu_1(3t/a)]^{1/2},$$

where μ_1 is the real part of the complex shear modulus of the bladder wall and associated tissues whose thickness is t, which probably is of the order $0{\cdot}2a$. The stiffness correction due to μ_1 is $(3t/a)$ times that used by Andreeva [6]. Using $t/a \simeq 0{\cdot}2$ gives $\mu_1 \simeq 2{\cdot}6 \times 10^6$ dynes/cm^2 for coalfish A and $\mu_1 = 3{\cdot}5 \times 10^5$ dynes/cm^2 for the pollack. Cod C apparently had a static excess pressure and μ_1 is less than $1{\cdot}4 \times 10^6$ dynes/cm^2. Andreeva quotes direct measurements of μ_1 in the region of 10^6 to 10^7 dynes/cm^2.

The ability of fish to withstand these sudden involuntary changes in depth seems to vary. Out of four coalfish, two had ruptured swimbladders at the surface; one exploded 2 ft from

the surface as it was being brought up by the diver who had previously killed the fish at depth and then watched the bladder expand. No haddock, *Melanogrammus aeglefinus* (L.), were caught during these experiments in 1968, but in previous years each one caught had a ruptured swimbladder at the surface. One out of two cod examined was ruptured, while the ling and pollack were intact. Ling have been observed to have bladders ballooning from their mouths when brought up from the depths in fishing nets. It is unlikely that the swimbladder wall is uniformly elastic, especially in view of the manner in which it is attached to the vertebral column, and it probably extends little in length and rather more in diameter to both static and dynamic pressures. From the above and other evidence [17], it is thus unlikely that the swimbladder volume and the external pressure follow Boyle's law, especially for fish brought to very shallow depths. A hypothetical characteristic is sketched in Figure 10 for a fish

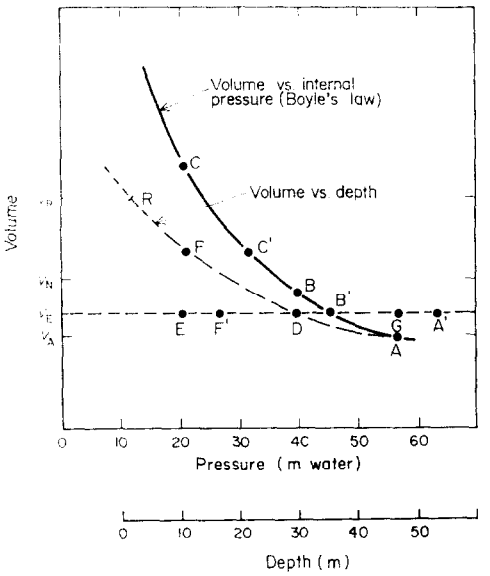

Figure 10. Hypothetical depth, volume characteristic for a stiff swimbladder (see text for explanation).

initially settled at 30 m depth. Without the tension of the walls, the mass of gas would occupy the volume at B, and the curve ABC is the isothermal gas characteristic for constant mass. With tension in the swimbladder wall, the internal pressure exceeds the external pressure by DB^1 and the volume is reduced to V_E so that the gas conditions are at B^1. If now the fish is placed deeper, not having time to absorb or secrete gas, the excess pressure will gradually drop to zero and the walls become flaccid, as at A. For further increases in depth, the volume V and external pressure will follow the gas law. If, instead, the fish is raised from 30 to 10 m depth, the bladder will come under greater stress, the volume increasing and the pressure decreasing to the point C^1. The excess pressure is now FC^1 which exceeds DB^1. The curve ADFR is the volume/depth characteristic, rupture possibly occurring at R just before atmospheric pressure is reached externally. The neutral buoyancy volume, V_N, which is essentially constant at all depths for a given fish, may be exceeded by the time the surface is reached; live swimbladder fish brought to the surface often float. Given time, the fish could presumably secrete gas to reach A^1 or absorb gas to reach F^1 and regain its volume V_E such that $GA^1 = EF^1 = DB^1$. The stiffness of the swimbladder characteristic in Figure 10 has been made high in order to separate the two curves for illustration purposes, and the relative values of V_R, V_N, V_E and V_A are speculative. The possession of a fairly stiff swimbladder by the fish has obvious advantages with regard to depth stability, and the low buoyancy helps to increase the vertical

range of a fish. Whilst low buoyancy has rarely been reported [17], it is evident that observations on live fish in shallow aquaria, or on fish brought up to the surface from deep water, are difficult to apply to the fish at depth. With refinements, the technique evolved here may be used by fish physiologists to obtain independent estimates of swimbladder volume in live experimental fish *in situ*. Fish audiologists from the Marine Laboratory, Aberdeen, have already used the technique to monitor the swimbladder condition before hearing tests.

Allowing for the measured values of D_T, the volumes of the swimbladder of coalfish A and the pollack at 30 m depth can be estimated from the surface dimensions to be 4·6 cm^3 and 5·5 cm^3, respectively. In view of the strong attachment to the rigid backbone, the length is probably constant with depth, so that the reduced volumes are achieved with slightly larger aspect ratios of 8·2 for the coalfish and 12 for the pollack; the resonant frequencies calculated from equation (2) must thus be increased by 20 and 28 % to 898 and 791 Hz compared with the measured values of 950 and 766 Hz, respectively. These discrepancies of −6 and +3 % are well within the experimental errors. Cod swimbladders have lower aspect ratios (e) [18] than coalfish and pollack, which may partially account for the low value of $f_r L$ for cod C. Cod B and coalfish B were ruptured, which probably explains their high resonant frequencies. Though cod A escaped before it could be examined, it is evident from Figure 4 that it was either using gas or losing it from a rupture and may have been doing so for some time before the high resonant frequency was first measured. The ling was kept alive for use in audiogram experiments and subsequently lived a considerable time before release, so an intact bladder is assumed. In Table 1 the volumes of three swimbladders which were not examined have been calculated from values of f_r and D_T using

$$f_r = (1{\cdot}25/2\pi a)\sqrt{3\gamma(D_f + 10 + D_T)/\rho} \times 10^5, \tag{10}$$

which allows a 25 % increase for shape. These volumes determined from acoustic measurements range from 25 to 83 % of those which would be calculated for the neutrally buoyant standard fish shape. It should be noted that the length-to-weight relationships of fish are known to vary even within a species, depending upon season and condition of the fish.

The highest Q observed at 30 m was 3·5 for cod A, and the lowest values correspond to overdamped systems. In general, cod and ling had the lowest, and coalfish and pollack the highest, damping. Damping consistently increased as a fish was raised and consistently decreased if it was lowered. Damping is principally due to shear losses within the tissue of the swimbladder wall, especially when this wall is under tension, and to viscous losses between the surrounding fish materials of differing density in a local acoustic field having high particle velocities. The radiation and other losses [6, 7, 19] are negligible in comparison with the fish tissue losses. According to Andreeva [6], the tissues can be characterized by a complex shear modulus $\mu_0 = \mu_1(1 + j\mu_2)$, in which case the tissue damping, for a spherical bladder completely surrounded by the viscoelastic material of thickness greater than the bladder dimensions, is

$$\delta_f = 4\mu_1\mu_2/(3\gamma P + 4\mu_1). \tag{11}$$

Our calculations (Appendix II) based on a thin-walled spherical viscoelastic shell, allowing for possible excess static pressure, give at resonance

$$\delta_f = \mu_2 . D_t/(D_f + 10 + D_s + D_t) = Q^{-1}. \tag{12}$$

Whilst either equations (11) or (12) would both predict the observed reduction of Q as the fish is raised and *vice versa*, the values of μ_2 necessary to explain the high damping are an order of magnitude larger than in [6] for other fish, though approaching values for a plastic material [26]. No allowance has been made for viscous losses in the other body parts, which will not be depth dependent and which the single experiment with the pollack showed to be significant. The damping must also be higher for an elongated bladder than for a spherical one. Since

the accuracies of the measurements are not very great, there is little point in pursuing these aspects further.

6. MEASUREMENTS AT HIGHER FREQUENCIES

The back-scattering cross-sections of the same and other live fish at higher frequencies were measured using a different method. An array of four transducers, mechanically resonant at 6·5 kHz, was used as a sound source over the band 4–20 kHz. Short pulses 1 msec long were transmitted at a frequency which was changed at third-octave intervals. The source was placed just below the surface and vertically above the live fish, which was contained at 30 m depth in a large polythene bag about 1 m long and 40 cm diameter; the fish could swim around in this bag, which was holed to allow respiration. In the same vertical line at 20 m depth an omnidirectional hydrophone was positioned between the sound source and the fish.

The incident and scattered pulses, separable in time, were received by the hydrophone and recorded via the same tuned amplifier on the same Polaroid film from a C.R.O. trace. In this way, the ratio of the incident and reflected pressures can be measured directly from the film, together with the setting of a calibrated attenuator switched into circuit during reception of the larger incident pulse; the ratio of the pulse amplitudes is independent of source levels, hydrophone sensitivity, amplifier and C.R.O. gains and frequency responses. The acoustic back-scattering cross-section is then determined from

$$\sigma = 4\pi[d_f(d_s + d_f)/d_s]^2 (v_s/v_i)^2, \tag{13}$$

where d_f and d_s are the distances from the hydrophone to the fish and sound source, respectively, and v_s and v_i are the scattered and incident pulse voltages. It is considered important that this method of absolute measurement of σ is not dependent upon standard or reference targets. The distances were known to $\pm 1\%$ but could have been measured by the pulse travel times.

The directions of the pulses incident on the fish and hydrophone differed by less than $1\frac{1}{2}°$, so that even at the highest frequency the error in v_i due to the directivity of the transmitting transducer is less than 0·6 dB. At each frequency, the value of v_i was very steady from pulse to pulse. Due to movement of the fish within the bag, the angle between the incident wave and the scattered wave as observed at the hydrophone could vary between 3 and $6\frac{1}{2}°$, and the incident wave may vary from 0 to 2° from the vertical. Also the live fish can pitch an unknown angle during the experiment and the major acoustic reflectors in the fish may be tilted relative to the mean horizontal axis of the fish [18] so that the angles of vertical incidence, dorsal aspect and maximum back-scattering do not necessarily coincide. Thus, directivity and fish movements cause variations in v_s from pulse to pulse. The maximum value of v_s over eight pulses superimposed on the film was used. In most cases v_s was well above background level; in cases where the fish echo was detectable, but comparable with the noise or reverberation level, corrections were made on an energy basis; occasionally σ was too small for v_s to be detectable. It is estimated that errors in (v_s/v_i) and target strength do not exceed ±2dB, though there is no guarantee that the absolute maximum value in the pitch plane has been recorded, especially at high L/λ. Nevertheless, the values obtained are probably fairly representative of what would be measured by an echo sounder at sea. In a separate experiment looking at fluctuations over 25 pulses, a minimum spread of 2·7 dB at one frequency and a maximum spread of 14 dB at a higher frequency were observed, but the spread did not consistently vary with frequency and it is felt that more data on variability are needed.

In the range $0{\cdot}8 < L/\lambda < 16$, 199 measurements on six species of swimbladder fish indicate variability from frequency to frequency, fish to fish and day to day. Absolute values occur with a similar spread to those of other authors in Figure 1 and it is considered that an alternative presentation and some further data reduction might be worthwhile; two methods are

demonstrated. Values of σ/L^2 were first averaged in third-octave bands of L/λ and plotted as the "mean" in Figure 11, which also shows the maximum and minimum observed in each band. A few results for a mackerel, *Scomber scombrus* (L.), a non-swimbladder fish, fall well below the mean of the swimbladder fish; this offers support for the conclusion of other workers that the swimbladder is a major scattering component of fish in this band, though it is also possible that the mean density and acoustic impedance of mackerel are less than those for the body of a fish having a swimbladder.

All the measurements were then plotted as in Figure 12, normalizing σ by λ^2 instead of L^2 after Love [4], who remarks that this improves the presentation of the data. Of course the quality of the data is unaltered, but whilst the σ/L^2 plot illustrates the frequency dependence,

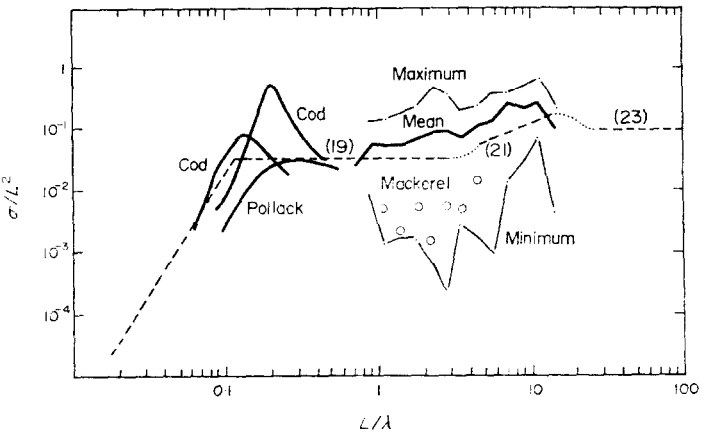

Figure 11. Summary plot of scattering normalized by length from fish in dorsal aspect at 30 m. Bracketed numbers refer to equations in the text.

the σ/λ^2 plot illustrates the fish-length dependence; it is apparent from the data that L is the more important parameter. A least mean-square regression of $10\log(\sigma/\lambda^2)$ on $10\log(L/\lambda)$ gave the line shown in Figure 12, for which the equation is

$$\sigma/\lambda^2 = 0{\cdot}029(L/\lambda)^{2{\cdot}45}. \tag{14}$$

Using equation (1), this can be re-written as

$$T = 24{\cdot}5\log_{10}L - 4{\cdot}5\log_{10}\lambda - 26{\cdot}4, \tag{15}$$

or

$$T = 24{\cdot}5\log_{10}L + 4{\cdot}5\log_{10}f - 27{\cdot}2, \tag{16}$$

where L and λ are in metres, f is kHz and T is in dB relative to 4π m^2, the cross-section of a perfectly reflecting sphere of radius 2 m. The 4·5 dB per decade increase with frequency is approximately the slope of the mean on Figure 11, as would be expected from the same data. The regression line is slightly lower in level than the arithmetic mean since it was obtained from $\log\sigma$ and thus is nearer a geometrical mean.

The data collated by Haslett [2] in Figure 1 has been replotted in Figure 13 as σ/λ^2 and the regression line obtained for these dorsal aspect data is

$$T = 25{\cdot}3\log_{10}L - 5{\cdot}3\log_{10}\lambda - 33{\cdot}4\,\text{dB}. \tag{17}$$

These results, equations (15) and (17), can be compared with those of Love, whose regression line for various fish in maximum *side* aspect is

$$T = 24{\cdot}1\log_{10}L - 4{\cdot}1\log_{10}\lambda - 23{\cdot}5\,\text{dB}. \tag{18}$$

There is close agreement on the length and frequency coefficients. The constant for maximum side aspect is 3 dB larger than our value for dorsal aspect, which is not unreasonable, since fish are generally deeper than they are broad. However, the difference in constants for

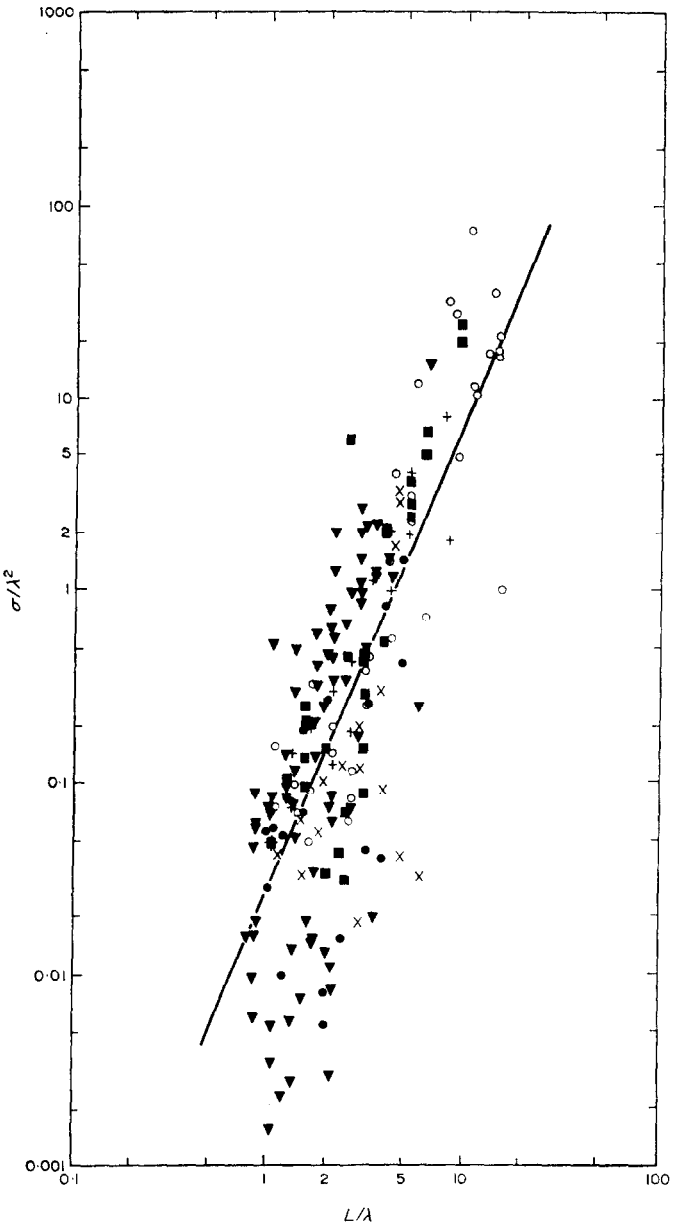

Figure 12. Results of scattering measurements on six species of fish, normalized by wavelength, and the regression line (——), equation (14). ▼, Coalfish; ×, ling; ●, cod; ■, haddock; o, pollock; +, whiting.

the two sets of dorsal data cannot be explained easily. Our data were obtained using *live* fish in good condition, the data of Figure 1 and equation (17) were from *dead* fish, some with artificial swimbladders. The higher coefficient of $\log_{10}L$ partially compensates for the difference in constants over the useful ranges of L and λ.

The individual points are by no means distributed normally about the regression line. In Figure 12 there are more points above and closer to the line than below it, suggestive of multiple scattering with broad maxima and deep interference minima. The standard error in the slope of Figure 12 is 1·4 dB/decade and the standard error of the constant is 0·7 dB.

Haslett [2] has calculated in some detail the contributions from various component structures of the fish using approximate geometrical shapes. We shall be content to calculate the contribution in several frequency bands from simple models representing the swimbladder

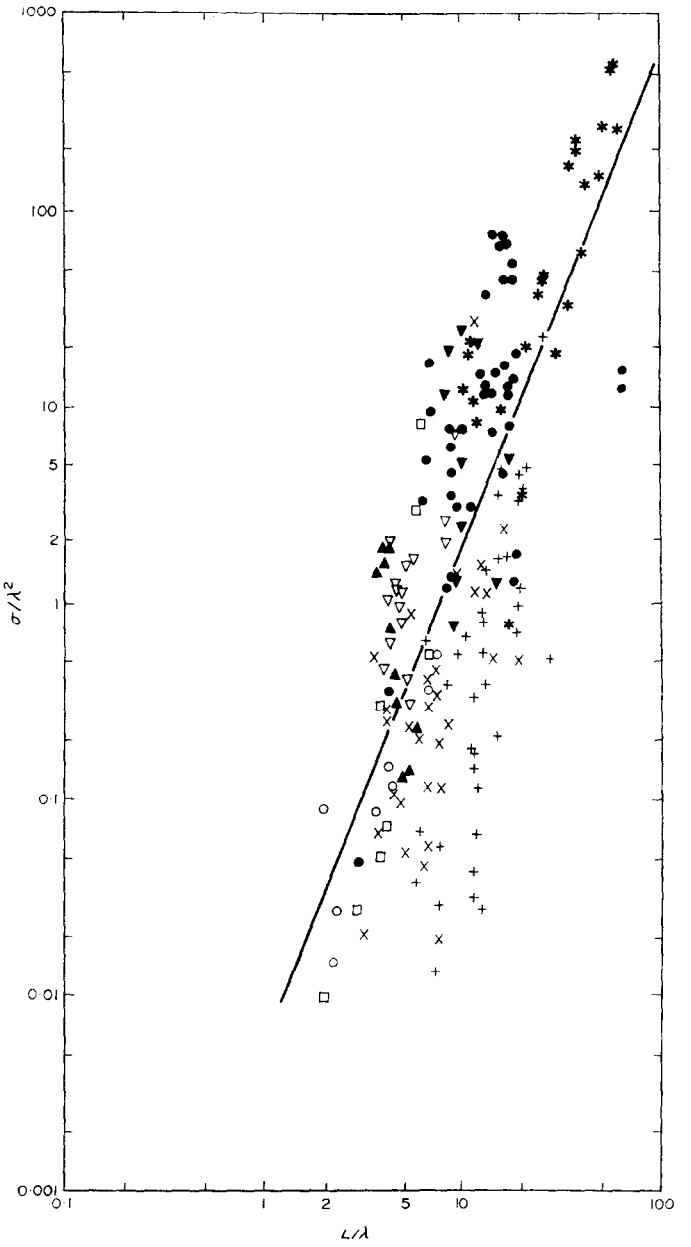

Figure 13. Results of scattering measurements by six authors on a wide variety of fish; data taken from Figure 1 and re-plotted normalized by wavelength instead of fish length. The regression line (——) is equation (17). □, Hashimoto; ▽, ▼, Sothcott; ●, Cushing; *, ×, +, Haslett; ▲, Jones and Pearce; o, Hashimoto and Maniwa.

for which the amplitude reflection coefficient, μ, can reasonably be taken as -1. Below resonance, the Rayleigh scattering region, σ is proportional to $L^6\lambda^{-4}$. Above resonance and below frequencies where the swimbladder dimensions are less than a wavelength, Weston [7] has shown that the acoustic cross-section is equal to the surface area for a soft spheroid of any aspect ratio. Thus a prolate spheroid of length $0{\cdot}36L$ and diameter $0{\cdot}036L$ would have

$$\sigma = 3 \times 10^{-2} L^2, \qquad f_r < f < 2{\cdot}8c_0/L. \tag{19}$$

The upper frequency limit is near $L/\lambda = 3$. Above this frequency, as first the swimbladder length and then other dimensions become comparable with a wavelength, the diffraction region is difficult to approximate simply. Modelling the swimbladder on a cylinder of length $l = 0{\cdot}36L$ and diameter $2b = 0{\cdot}03L$, the latter less than the prolate spheroid minor dimension in order to give the same volume, $2{\cdot}5 \times 10^{-4} L^3$, which is somewhat lower than neutral buoyancy volume in accordance with Table 1, we can use the scattering cross-section of a finite cylinder [20, 21]

$$\sigma = (2\pi b l^2/\lambda)\mu^2, \tag{20}$$

giving then

$$\sigma = 1{\cdot}2 \times 10^{-2} L^3/\lambda, \qquad 5{\cdot}3c_0/L < f < f_u. \tag{21}$$

The lower frequency limit is determined from $2\pi b/\lambda > \frac{1}{2}$, and corresponds to $L/\lambda > 5{\cdot}3$. It should be noted that equations (19) and (21) intersect at $L/\lambda = 2{\cdot}5$, so that it is reasonable for σ to be less than equation (21) and more than equation (19) in $2{\cdot}5 < L/\lambda < 5{\cdot}3$. The upper limit, f_u, of the finite cylinder approximation will depend upon the curvature of the long axis of the bladder, and at high frequencies scattering is specular. Using the laws of geometrical optics, Tucker and Stubbs [21] calculate that for an ellipsoid of length l, breadth $2b$, and depth $2c$,

$$\sigma = (\pi l^2 b^2/16c^2).\mu^2. \tag{22}$$

This arises because the two principal radii of curvature are $l^2/8c$ and $b^2/2c$. In this case of a prolate spheroid $b = c$, $\mu = -1$ and $\sigma = \pi l^2/16$, which, surprisingly, is independent of b and gives

$$\sigma = 10^{-1} L^2, \qquad f_u < f. \tag{23}$$

For this approximation to apply, $2b > \lambda$, and the lower limit will correspond to $L/\lambda > 28$. Since equations (21) and (23) intersect at $L/\lambda = 8$, σ is somewhat uncertain in the region $8 < L/\lambda < 28$. However, the geometrical optics approximation takes no account of surface creeping waves, which Senior [22] has shown can enhance high frequency scattering from prolate spheroids for "end" or "nose on" incidence. At all events the frequency range in which a 10 dB/octave slope can be expected is quite restricted, probably to less than the range over which the regression lines have been forced. Some more recent broadside measurements by Haslett [23] at high L/λ values show very low or zero frequency dependence. It is apparent in broad outline and general level, if not in precise detail, that the swimbladder can account for practically all the scattering from these fish. Higher values than these approximations can be expected if the fish is nearer neutral buoyancy, if the swimbladder is concave along its length, or if it is broader than it is deep.

Though the rest of the fish is bulkier than the swimbladder this is more than offset by the much reduced amplitude reflection coefficient, so that scattering is an order of magnitude at least below that from the bladder. There is some uncertainty about the value of μ for fish flesh and bone in sea water. Haslett [2, 24] has obtained $\mu = 0{\cdot}019$ by measurement at a high frequency on small samples of flesh, whilst Mahrous and Cushing [25] find a sound velocity in fish flesh of 1620 m/sec, which would give $\mu \simeq 0{\cdot}064$. For cod bone, Haslett measures $\mu = 0{\cdot}25$ to give $c_0 = 1280$ m/sec, whilst Mahrous and Cushing measure $c_0 = 5650$ m/sec, giving $\mu = 0{\cdot}76$.

7. CONCLUSIONS

(i) A technique has been developed whereby the swimbladder resonance of a live or dead fish may be observed and measured at sea.

(ii) Using this method, the resonant frequencies of several live gadoid fish were found to be higher than would be predicted for a neutrally buoyant fish with a spherical swimbladder.

(iii) The three major reasons for the higher frequency of resonance are (a) the elongation of the bladder, (b) an excess internal pressure due to the stiffness of the bladder wall and (c) the fact that apparently the bladders of the experimental fish were insufficiently inflated to provide neutral buoyancy.

(iv) The damping of resonance in all cases was high and was due in roughly equal measure to the losses in the bladder wall tissues and the gut beneath.

(v) Measurements on elongated balloons confirmed the validity of the resonance technique and showed that the effect of aspect ratio was close to the theoretical calculations of Weston [7].

(vi) Application of swimbladder resonance for the sizing of commercial fish at liberty in the sea is not a practical proposition due to severe and fundamental transducer and resolution limitations.

(vii) The *in situ* resonance technique described here is considered to be a valuable method of monitoring the swimbladder function.

(viii) An absolute method of measuring the target strength of fish at higher frequencies has also been developed; it does not depend upon calibrated transducers or upon "standard" targets.

(ix) Measurements in dorsal aspect on live fish in the range $0{\cdot}8 < L/\lambda < 20$ give an empirical equation,

$$T = 24{\cdot}5 \log_{10} L - 4{\cdot}5 \log_{10} \lambda - 26{\cdot}4$$

It is recommended that this equation be used when sizing by target strengths with calibrated echo sounders at sea.

(ix) The major cause of scattering over the whole frequency band is the swimbladder.

ACKNOWLEDGMENTS

The authors wish to thank the Director of the Marine Laboratory, Aberdeen, for placing *F.R.S. Mara* at their disposal; to the officers and crew of that worthy ship, grateful appreciation of much assistance and patience on station is recorded. It is a great pleasure to acknowledge the invaluable help from, and discussion with, C. J. Chapman, A. D. Hawkins and other biologists and divers, all from the Marine Laboratory, Aberdeen, without whose tremendous efforts the work would not have been possible. The assistance of a vacation student, D. K. Fryer, was appreciated and discussions with a colleague, M. J. Tucker, were most valuable.

REFERENCES

1. R. W. G. Haslett 1962 *J. Cons. perm. int. Explor. Mer.* **27**, 261. Measurement of the dimensions of fish to facilitate calculations of echo-strength in acoustic fish detection.
2. R. W. G. Haslett 1965 *Br. J. appl. Phys.* **16**, 1143. Acoustic back-scattering cross-sections of fish at three frequencies and their representation on a universal graph.
3. D. H. Cushing 1968 *Fishery Invest., Lond.* II **25** (10). The abundance of hake off South Africa.
4. R. H. Love 1969 *J. acoust. Soc. Am.* **46**, 746. Maximum side-aspect target strength of an individual fish.
5. J. B. Hersey and R. H. Backus 1954 *Deep Sea Res.* **1**, 190. New evidence that migrating gas bubbles, probably the swimbladders of fish, are largely responsible for scattering layers on the continental rise south of New England.

6. I. B. ANDREEVA 1964 *Akust. Zh.* **10**, 20 (*Sov. Phys. Acoust.* **10**, 17). Scattering of sound by air bladders of fish in deep sound-scattering ocean layers.
7. D. E. WESTON 1967 In *Underwater Acoustics* (Ed. V. M. Albers). New York: Plenum Press. Vol. 2, Chap. 5, Sound propagation in the presence of bladder fish.
8. R. P. CHAPMAN and J. R. MARSHALL 1966 *J. acoust. Soc. Am.* **40**, 405. Reverberation from deep scattering layers in the western North Atlantic.
9. B. S. MCCARTNEY, A. R. STUBBS and M. J. TUCKER 1965 *Nature, Lond.* **207**, 39. Low-frequency target strengths of pilchard shoals and the hypothesis of swimbladder resonance.
10. B. S. MCCARTNEY 1967 In *Underwater Acoustics* (Ed. V. M. Albers). New York: Plenum Press. Vol. 2, Chap. 10, Underwater sound in oceanography.
11. W. C. HODGSON 1950 *Fishery Invest., Lond.* II **17** (4). Echo-sounding and the pelagic fisheries.
12. R. BALLS 1947 *J. Cons. perm. int. Explor. Mer* **15** (2), 193. Herring fishing with the echometer.
13. E. C. LA FOND 1965 *NEL Rep.* 1342, 49. Oceanographic research tower.
14. H. O. BERKTAY, J. R. DUNN and B. K. GAZEY 1968 *Appl. Acoust.* **1**, 81. Constant beamwidth transducers for use in sonars with very wide frequency bandwidths.
15. D. G. TUCKER and N. J. BARNICKLE 1969 *J. Sound Vib.* **9**, 393. Distinguishing automatically the echoes from acoustically "hard" and "soft" objects with particular reference to the detection of fish.
16. M. HUND and H. KUTTRUFF 1962 *Acustica* **12**, 404. Pressure-chamber method of measurement of acoustical impedances of small bodies (hydrophones) in liquids.
17. R. MCN. ALEXANDER 1966 *Biol. Rev.* **41**, 141. Physical aspects of swimbladder function.
18. L. MIDTTUN and I. HOFF 1962 *FiskDir. Skr., Havundersøkelser* **13**, 3. Measurements of the reflection of sound by fish.
19. C. DEVIN JR 1959 *J. acoust. Soc. Am.* **31**, 1654. Survey of thermal, radiation and viscous damping of pulsating air bubbles in water.
20. R. W. G. HASLETT 1964 *Br. J. appl. Phys.* **15**, 1085. The acoustic back-scattering cross-sections of short cylinders.
21. M. J. TUCKER and A. R. STUBBS 1958 *Nat. Inst. Oceanogr. intern. Rep. A.*12. The reflection of sound by fish.
22. T. B. A. SENIOR 1966 *Can. J. Phys.* **44**, 655. The scattering from acoustically hard and soft prolate spheroids for axial incidence.
23. R. W. G. HASLETT 1969 *J. Sound Vib.* **9**, 181. The target strengths of fish.
24. R. W. G. HASLETT 1962 *Proc. Phys. Soc.* **79**, 559. The back-scattering of acoustic waves in water by an obstacle, II: Determination of the reflectivities of solids using small specimens.
25. M. A. MAHROUS and D. H. CUSHING, Personal communication.
26. G. WORKMAN and S. I. HAYEK 1969 *J. acoust. Soc. Am.* **46**, 1340. Transmission of acoustic waves through submerged viscoelastic spherical shells.
27. A. E. H. LOVE 1927 *Mathematical Theory of Elasticity*. London: Cambridge University Press, 4th Ed., Art 98.

APPENDIX I

HYDROPHONE SENSITIVITIES AND CALIBRATION CONSTANT

In order to convert the uncalibrated plots of Figures 3, 5, 6, 7 and 8, it is necessary to know the hydrophone sensitivities S_s and S_p and hence the calibration factor of equation (7),

$$20 \log_{10} (R.S_p/S_s).$$

It was not possible to calculate theoretically the sensitivities with any confidence owing to the complex boundary conditions. The edge-on sensitivity to plane waves, S_p, was determined (see Figure A1) by a conventional substitution calibration. To obtain S_s, a small piezo-electric sphere was placed at the centre of the ring and used as a transmitter over the frequency band 100 Hz–10 kHz. The voltages from the ring and another small calibrated hydrophone some distance away in the far field were measured. The ring sensitivity was therefore obtained, (Figure A1) relative to the hydrophone for spherical waves originating at the centre of the ring and referred to far field although $R \ll \lambda$. The resulting factor (Figure A1) has been used in Figure 8 for the nearly spherical balloon and the measured target strength is very close to

the theoretical values for a Q of 10. Application of the calibration factor to the elongated balloons and the fish is less certain. Well away from the scatterer, the field is spherical since it is a monopole smaller than a wavelength, and high order vibrational modes have inefficient radiation. However, at the position of the ring, which is separated from the scatterer by the same order as the length of the scatterer, the field is more complex and a proximity correction

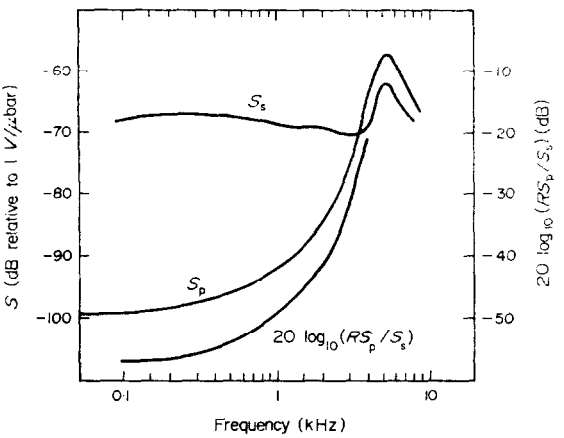

Figure A1. Measured sensitivities of ring hydrophone. S_s to spherical waves from the centre of the ring, S_p to "edge-on" plane waves. $20\log_{10}(RS_p/S_s)$ is the calibration term in equation (7).

might be necessary, depending upon the aspect ratio. The calibration factor, uncorrected, was applied to the cod which had the highest Q, the pollack having the lowest Q, and another cod with the lowest normalized frequency, all plotted in Figure 11. Taking account of the higher resonant frequency discussed above in section 6, the calibrated and normalized results at low frequencies on Figure 11 fit the theoretical values of equation (19) and the Rayleigh scattering below resonance sufficiently closely to suggest that any corrections due to the proximity of the ring are small.

Radial and axial displacements of the target from the centre of the ring were shown to have no effect on the resonant frequency and a small effect on amplitude so that, providing the ring is placed around the bladder, further accuracy in positioning is unnecessary.

APPENDIX II

THE EFFECTS OF SWIMBLADDER TISSUE ON RESONANCE

For simplicity, the fish is modelled on a spherical viscoelastic shell (swimbladder) surrounding a gas volume V and surrounded by an infinite body of water. If the shell density is the same as water the radiation load on the bladder is the same as that on a spherical bubble of the same size, but the mechanical stiffness is altered due both to an increased internal static pressure and to elastic energy storage in the shell, and the damping is increased due to incomplete recovery of stored energy within the shell.

The radial displacement of a spherical elastic shell is given [27] by

$$U_r = \frac{1}{3B}\cdot\left(\frac{p_1 r_1^3 - p_0 r_0^3}{r_0^3 - r_1^3}\right).r + \frac{1}{4\mu_0}\cdot\left(\frac{r_0^3 r_1^3 (p_1 - p_0)}{r_0^3 - r_1^3}\right)\cdot\frac{1}{r^2},$$

where p_1 and p_0 are the internal and external pressures at radii r_1 and r_0, respectively, B is the bulk modulus of compressibility, μ_0 is the shear modulus and $r_1 \leqslant r \leqslant r_0$. For viscoelastic materials, B is taken to be real, and μ_0 is complex and frequency dependent [26]. Andreeva [6]

defined $\mu_0 = \mu_1(1 + j\mu_2)$ and considered the bladder material to have dimensions larger than the bladder, so that putting $p_0 = 0$ at $r_0 \to \infty$ gives

$$U_{r_1} = p_1 . r_1/4\mu_0.$$

However, this approximation does not seem too satisfactory in view of the experiment in which the gut below the pollack was removed, causing decreased damping but not affecting the resonant frequency. Let the wall be thin so that $r_0 - r_1 = t$ and $(r_0^3 - r_1^3) \simeq 3r_1^2\, t$ giving

$$U_{r_1} \simeq (p_1 - p_0) . \frac{r_1^2}{3t} . \left(\frac{1}{3B} + \frac{1}{4\mu_0}\right).$$

It is probable that, like natural rubber [26], $B \gg \mu_0$ for the bladder wall tissue, giving

$$U_{r_1} \simeq (p_1 - p_0) . \frac{r_1}{4\mu_0} . \left(\frac{r_1}{3t}\right),$$

which indicates an extension $(r_1/3t)$ times that produced by Andreeva's approximation. Now if the bladder is initially extended U beyond the flaccid state, then the excess internal pressure is $\Delta P = 4\mu_1 . 3tU/r_1^2$ where it has been assumed that $\mu_2 = 0$ at zero frequency. Devin [19] and Weston [7] derive formulae for the resonant frequency and damping of gas bubbles, and Weston [7] and Andreeva [6] discuss damping coefficients due to fish tissue, so that it is not necessary to write down the derivation here in full, except to point out that the difference between the gas pressure and the sum of the incident and scattered pressures at the radius a must equal $4\mu_0 . 3tu_a/a^2$ instead of zero, where u_a is now the acoustic displacement of the wall and $a = r_1 + U$. The resonant frequency is then given by

$$f_r = (2\pi a)^{-1} . \rho^{-1/2} . \left[3\gamma(P + \Delta P) + 4\mu_1 . \frac{3t}{a} . (1 - k_0 a\mu_2)\right]^{1/2},$$

the damping by

$$\delta = \delta_r + \delta_f,$$

where δ_r, the radiation damping is $ka . \omega_0^2/\omega^2$ and the tissue damping is

$$\delta_f = \frac{4\mu_1 \mu_2}{\rho\omega^2 a^2} . \frac{3t}{a}.$$

Now $k_0 a\mu_2 \ll 1$ so that we obtain

$$f_r = (2\pi a)^{-1} . \rho^{-1/2} . \left[3\gamma P + 12\mu_1 t . \left(\frac{3\gamma U}{(a-U)^2} + \frac{1}{a}\right)\right]^{1/2},$$

or, if Andreeva's assumption was used,

$$f_r = (2\pi a)^{-1} \rho^{-1/2} \left[3\gamma P + 4\mu_1 \left(\frac{3\gamma U}{(a-U)} + 1\right)\right]^{1/2},$$

which reduces to her formula if $U = 0$.

It is interesting to note that in the case of a small gas bubble for which surface tension σ_t is significant,

$$f_0 = (2\pi a)^{-1} . \rho^{-1/2} . [3\gamma(P + 2\sigma_t/a) - 2\sigma_t/a]^{1/2}.$$

The term $+2\sigma_t/a$ is the static excess internal pressure, but the term $-2\sigma_t/a$ is a consequence of σ_t remaining constant as the bubble oscillates, so that during the expansion cycle the total excess internal pressure is being reduced.

Returning to the experiment in which f_r is measured as the fish depth is altered, and if μ_1 is in dynes/cm^2, the apparent excess pressure in terms of metres of water is given by

$$D_T = (3\gamma)^{-1} \times 10^{-5} . 12\mu_1 t \left(\frac{3\gamma U}{(a-U)^2} + \frac{1}{a}\right).$$

That is,

$$D_T = D_s + D_t,$$

where the static excess head of water is

$$D_s = 12\mu_1 \frac{t.U}{(a-U)^2} \times 10^{-5},$$

and the effective contribution due to tissue rigidity is

$$D_t = 4\mu_1 \frac{t}{\gamma a} \times 10^{-5}.$$

$D_s = D_t$ if $U/a \sim 0{\cdot}2$, which is a large strain but not an impossible one for the fish raised from 30 to 10 m. For a fish forced to undergo rapid changes in depth, U will change and though this could be calculated, it requires the assumption of linear elasticity, which is doubtful since a large proportion of bladders ruptured. If a plot of $f_r^{1\cdot2}$ *versus* D_f is a straight line then it suggests that $U = 0$ over the range of D_f, that $D_s = 0$ and that $D_T = D_t$.

At resonance, the tissue damping is

$$\delta_f = \mu_2 D_t/(D_f + 10 + D_t + D_s).$$

μ_2 is probably frequency dependent.

These calculations based on a spherical bladder can only serve as a guide to the real fish, whose swimbladder is, in general, a more complex shape and stiffened by the vertebrae, whose tissues do not have uniform thickness or elastic properties and whose recent pneumatic history is so important.

APPENDIX III

NOMENCLATURE

- a radius of bubble or swimbladder
- B bulk modulus of tissue
- $2b$ diameter of cylinder or breadth of ellipsoid
- $2c$ depth of ellipsoid
- c_0 velocity of sound
- D_f depth of fish
- D_s actual excess static pressure in metres of water
- D_T equivalent total excess internal pressure in metres of water
- D_t equivalent excess pressure due to tissue elasticity
- d_f distance between hydrophone and fish
- d_s distance between hydrophone and source
- e ratio of length to diameter for prolate spheroid
- f frequency
- f_e resonant frequency of spheroid
- f_0 resonant frequency of spherical bubble
- f_r resonant frequency of fish swimbladder
- f_u upper frequency limit of cylindrical approximation
- L length of fish
- l length of cylinder or ellipsoid
- P absolute static pressure
- ΔP excess static pressure
- p_i incident acoustic pressure
- p_s scattered acoustic pressure
- Q ratio of resonant frequency to 3 dB bandwidth
- r radius of shell
- R radius of ring hydrophone, distance from fish
- S_p sensitivity of ring hydrophone to "edge-on" plane waves
- S_s sensitivity of ring hydrophone to spherical waves

t thickness of tissue
T target strength
U initial radial displacement of spherical bladder
u_a acoustic displacement of bladder wall
V volume of swimbladder
V_E original volume of bladder before change in depth
V_N neutral buoyancy volume
V_R volume of bladder at rupture
v hydrophone voltage
v_1 ring hydrophone voltage with fish present
v_2 ring hydrophone voltage without fish
v_i incident pulse voltage
v_s scattered pulse voltage
γ ratio of specific heats of gas
δ damping factor
δ_f damping factor at resonance due to fish tissue
δ_r damping factor at resonance due to acoustic radiation
λ wavelength
μ amplitude reflection coefficient
μ_0 $= \mu_1(1 + j\mu_2)$ complex shear modulus of tissue
ρ density
σ acoustic back-scattering area
σ_t surface tension
ω $= 2\pi f$